Hydrogen sulfide-mitigated salinity stress impact in sunflower seedlings was associated with improved photosynthesis performance and osmoregulation

Abeer Abdelrazk Younis[1] and Mohamed Magdy Fahim Mansour[1*]

Abstract

Background Salinity is one major abiotic stress affecting photosynthesis, plant growth, and development, resulting in low-input crops. Although photosynthesis underlies the substantial productivity and biomass storage of crop yield, the response of the sunflower photosynthetic machinery to salinity imposition and how H_2S mitigates the salinity-induced photosynthetic injury remains largely unclear. Seed priming with 0.5 mM NaHS, as a donor of H_2S, was adopted to analyze this issue under NaCl stress. Primed and nonprime seeds were established in nonsaline soil irrigated with tape water for 14 d, and then the seedlings were exposed to 150 mM NaCl for 7 d under controlled growth conditions.

Results Salinity stress significantly harmed plant growth, photosynthetic parameters, the structural integrity of chloroplasts, and mesophyll cells. H_2S priming improved the growth parameters, relative water content, stomatal density and aperture, photosynthetic pigments, photochemical efficiency of PSII, photosynthetic performance, soluble sugar as well as soluble protein contents while reducing proline and ABA under salinity. H_2S also boosted the transcriptional level of ribulose 1,5-bisphosphate carboxylase small subunit gene (*HaRBCS*). Further, the transmission electron microscope showed that under H_2S priming and salinity stress, mesophyll cells maintained their cell membrane integrity and integrated chloroplasts with well-developed thylakoid membranes.

Conclusion The results underscore the importance of H_2S priming in maintaining photochemical efficiency, Rubisco activity, and preserving the chloroplast structure which participates in salinity stress adaptation, and possibly sunflower productivity under salinity imposition. This underpins retaining and minimizing the injury to the photosynthetic machinery to be a crucial trait in response of sunflower to salinity stress.

Keywords Chloroplast, Hydrogen sulfide, Photosynthesis, Rubisco, Salinity, Sunflower

*Correspondence:
Mohamed Magdy Fahim Mansour
mfmansour@sci.asu.edu.eg; mf_mansour@yahoo.com
[1]Faculty of Science, Department of Botany, Ain Shams University,
Cairo 11566, Egypt

Background

Among numerous abiotic stresses, salinity stress is a major abiotic constraint threatening global food security by decreasing agricultural productivity and a major hurdle in accomplishing the "zero hunger" goal proposed by FAO-UN [1]. Salinity stress is drastically increasing due to anthropogenic activities (i.e., irrigation malpractice, fertilization…etc.) and natural causes like soil salinization and poor water quality [2, 3]. Approximately 1.5 million hectares of farmland representing around 33% of irrigated land have been affected by salinity [4] and are predicted to climb up to a staggering 50% by 2050 [5]. Salinity stress involves ionic and osmotic stresses: osmotic stress is the first stress experienced when a plant is exposed to saline soil while ionic stress occurs later when salt levels reach a threshold beyond which the plant cannot maintain ion homeostasis and growth [6]. Both osmotic and ionic action of salinity ultimately cause oxidative stress affecting various physiological and biochemical processes in plants [7, 8], which eventually drastically impacts overall plant growth, development, metabolism, and productivity [9]. In addition, the changing climatic conditions and their effects on farming worsen the salinity problem and further threaten the stability of agricultural production. Therefore, addressing the salinity problem will be necessary for the future, given the growing population of the planet and the ever-increasing demand for food, which necessitate developing salinity-resilient crops required for sustainable agriculture and global food security.

Photosynthesis is the major source of energy that has significant implications on the redox status of plant cells and hence regulates all aspects of plant metabolism and physiology [10]. Therefore, the evaluation of the pivotal role of photosynthesis in plant phenotyping under stressful conditions is a very important task. Sarabi et al. [11] report that salinity stress exerts detrimental effects on photosynthesis, manifested through stomatal and non-stomatal limitations. Stomatal limitation refers to stomatal closure resulting in inefficient gas exchange and reduced photosynthetic rate [12, 13]. Non-stomatal limitations, mainly associated with the degradation of pigment-protein complexes, destruction of fine thylakoid membrane structure [14], reduction in PSII photochemical efficiency (F_v/F_m) [15], and decreased activity of ribulose 1,5-bisphosphate carboxylase/oxygenase (Rubisco) [16, 17]. Plant photosynthetic efficiency has been reported to be a reliable, non-destructive biomarker for determining the salinity tolerance of wheat genotypes [18]. It is also reported that the expression of the small subunit regulates the size of the Rubisco pool in plants and can influence the overall catalytic efficiency of the Rubisco complex [19]. Additionally, chlorophyll and carotenoids play a fundamental role in photosynthesis by capturing light energy and inducing electron transfer, and changes in their levels are related to the efficiency of the photosynthetic machinery under salinity stress [20, 21]. Therefore, the analysis of plant photosynthetic efficiency based on measurements of various photosynthetic parameters (photosynthetic performance (PI_{abs}), the maximal quantum yield of PSII photochemistry (F_v/F_m), Chlorophyll a, chlorophyll b, carotenoids, and Rubisco small subunit expression) is an accurate approach for evaluating plant responses to unfavorable photosynthesis environmental conditions and their impact on crop plants [11, 17, 22].

Sunflower (*Helianthus annuus* L.) has great importance in the world economy as one of the most cultivated oilseed crops; the seed oil content ranges between 38 and 50% and is widely used in human food and the production of biodiesel [23, 24]. Also, sunflower seeds are a rich nutritional source, boasting high levels of protein, fiber, minerals, and phenolic compounds [25]. The cultivated area of sunflower in Egypt is tiny, although edible oil production is still deficient for population demand, with only 5% of the total oil demand covered by domestic production [26]. Therefore, increasing the domestic oil yield of sunflower is in demand and could be adopted by increasing the cultivated area, which may impose the use of saline soils, parallel to exploring the strategies for enhancing salinity tolerance of sunflower and promoting its production under this adverse conditions [26]. One of the short-term and most pragmatic approaches to boosting plant resistance to salinity is seed priming. Seed priming is a cost-effective eco-friendly technique that might have an enormous impact on oilseed production and sustainable agriculture and food security problems [27–29]. H_2S, an emerging gaseous signaling molecule in plants, plays a pivotal role in regulating various physiological, biochemical, and developmental processes, including seed germination, plant growth, and development, regulates stomatal apertures, promotes photosynthetic activity, enhances plant's resistance to abiotic stresses [30–33]. H_2S as a signaling molecule in plants regulates these processes through crosstalk with other signaling molecules resulting in the repairing of biomembranes and denatured proteins as well under stress [34]. As a result, we hypothesized that the H_2S priming to sunflower seeds could boost stomatal mechanics and protect the stability of chloroplast structure and photosynthetic pigments, which in turn, could enhance photosynthetic efficiency. Therefore, seed priming with NaHS (H_2S donor) was adopted to analyze this approach's efficiency in overcoming the negative adversities of salinity stress on sunflower photosynthesis. This is because how H_2S stimulates sunflower salinity resilience in terms of photosynthetic apparatus performance remains largely unclear. To answer this question, we investigated the

impact of H_2S priming on photosynthetic parameters, Rubisco small subunit gene expression, chloroplast ultrastructure, and stomatal movement in sunflower seedlings under salinity stress, aiming to provide insights into its potential mitigation role on photosynthetic machinery of NaCl-stressed sunflower seedlings. This might participate in improving sunflower adaptation to salinity stress, and hence productivity under salinity imposition.

Results

NaCl stress reduced sunflower seedlings' growth in terms of plant fresh weight, dry weight, and leaf area, while increasing the root-to-shoot ratio (R/S ratio) (Fig. 1b-e). However, H_2S priming significantly enhanced the growth of NaCl-stressed and non-stressed sunflower seedlings and reduced the R/S ratio in stressed seedlings relative to their corresponding controls (Fig. 1b-e). There is no significant difference in plant height and leaf number among treatments (Fig. 1a, f).

For stomatal characteristics, normal epidermal cells with stomata exhibited proper shape and open aperture
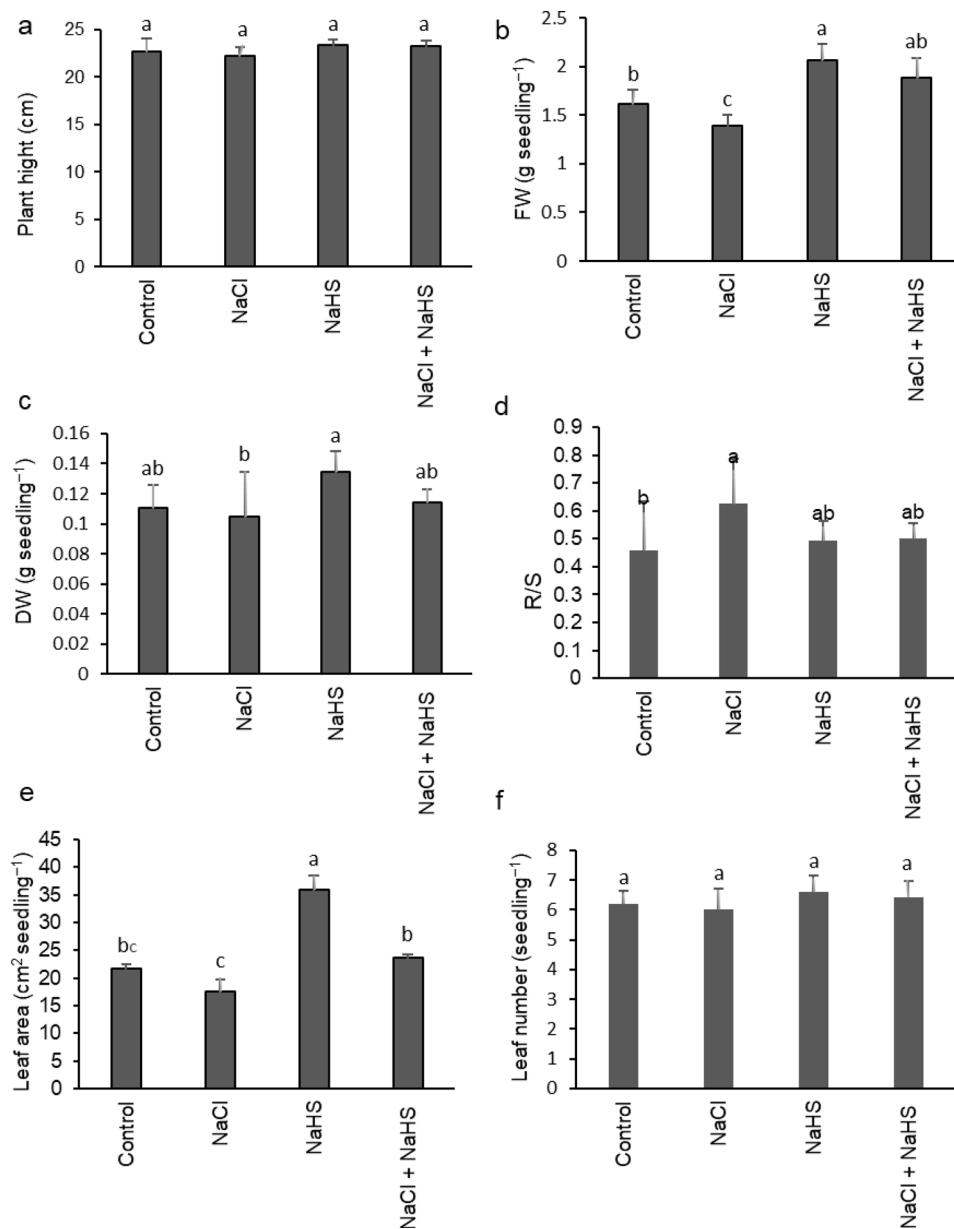

Fig. 1 Effect of NaHS priming in the presence and absence of 150 mM NaCl on (**a**) plant height, (**b**) fresh weight (FW), (**c**) dry weight (DW), (**d**) root/shoot ratio (R/S), (**e**) leaf area, and (**f**) leaf number of sunflower seedlings. Each value is the mean ± SD of three replicates. Bars with different letters indicate significant differences at $P \leq 0.05$
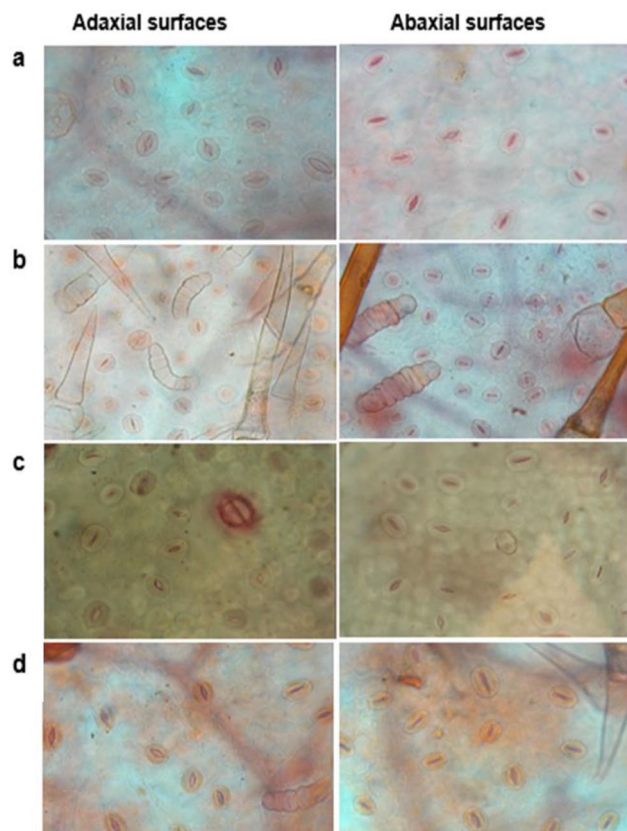
Fig. 2 Effect of NaHS priming on stomatal characteristics of sunflower seedlings leaves in the presence and absence of 150 mM NaCl. (**a**) control, (**b**) NaCl, (**c**) NaSH, and (**d**) NaCl + NaSH

in both adaxial and abaxial surfaces were observed in control and H_2S alone treatments, (Fig. 2a, c). However, leaves of salinity-treated seedlings showed deformed guard cells, shrink epidermal cells, decreased stomatal size, closed apertures, as well as the presence of trichomes of thorn-like outgrowths (Fig. 2b). Plants received H_2S priming and NaCl stress showed relatively normal shaped guard cells with partially opened stomatal aperture (Fig. 2d). Data presented in Table 1 revealed that several epidermis and stomata of salinity-stressed

sunflower leaves significantly decreased by 22.5% and 22.3% for the adaxial surface and by 26.9% and 29.6% for the abaxial surface, respectively, compared with the control plants. Stomatal indices of adaxial and abaxial surfaces of salinity-stressed leaves significantly reduced by 26.2% and 20.7%, respectively, relative to the control ones (Table 1). Also, the reduced stomatal width and length in the salinity-treated plants resulted in a significantly reduced stomatal area of adaxial and abaxial surfaces (Table 1). The highest decrease in the stomatal area was observed on the abaxial surface (40%) of salinity-stressed leaves compared with the control (Table 1). On the other hand, H_2S priming alleviated salinity-induced reductions in stomatal number, sizes, and stomatal indices of both surfaces of stressed leaves. The H_2S-positive impacts were also observed in the non-stressed leaves (Table 1).

Exposure of sunflower seedlings to NaCl stress significantly increased the content of ABA by 248.7% and 335.6% in the shoots and roots, respectively, relative to their controls (Fig. 3a). H_2S priming significantly reduced ABA content by 43.5% and 45.1% in the shoots and roots, respectively, compared with those received only NaCl stress (Fig. 3a). Salinity stress also remarkably decreased the LRWC by 29.3% in salinity-stressed seedlings relative to unstressed ones, whereas H_2S priming significantly restored LRWC to the control value or even higher in stressed and non-stressed conditions (Fig. 3b).

The chloroplast ultrastructure of the control and H_2S-primed leaves exhibited ellipsoid shape with compactly arranged thylakoids and well-compartmentalized grana stacks with distinct grana lamellae (Fig. 4a, c), while under salinity stress, the chloroplast appeared rounded and displayed a disrupted envelope with a disorganized outer membrane, and loosened grana lamella with distorted thylakoid (Fig. 4b). However, H_2S pretreatment alleviated the above salinity-induced ultrastructure disorders as distinct chloroplast membrane envelope, and a more regular arrangement of stroma thylakoids were observed compared with the samples received only NaCl stress (Fig. 4d).

Table 1 The structure of the adaxial and abaxial epidermis in leaves of sunflower seedlings pretreated with NaHS, donor of H_2S, in the presence and absence of 150 mM NaCl

	Treatment	Epidermal cells number (mm²)	Stomatal number (mm²)	Stomatal index	Stomatal length (μm)	Stomatal width (μm)	Stomatal area (μm²)
Adaxial surfaces	Control	107.50 ± 2.17[b]	37.33 ± 1.39[a]	25.77 ± 0.77[a]	20.30 ± 0.2[ab]	1.80 ± 0.14[b]	29.0 ± 1.67[b]
	NaCl	83.33 ± 0.64[d]	29.0 ± 0.97[c]	19.03 ± 0.64[c]	15.70 ± 0.15[c]	1.10 ± 0.10[d]	19.0 ± 1.44[d]
	NaHS	111.33 ± 3.16[a]	37.0 ± 1.03[ab]	25.15 ± 0.53[ab]	22.90 ± 0.35[a]	1.90 ± 0.2[a]	33.0 ± 1.89[a]
	NaCl + NaHS	96.66 ± 1.77[c]	34.33 ± 1.3[b]	23.0 ± 0.35[b]	19.60 ± 0.18[b]	1.30 ± 0.17[c]	24.0 ± 1.52[c]
Abaxial surfaces	Control	99.16 ± 1.18[b]	56.33 ± 1.59[ab]	36.23 ± 0.98[ab]	18.90 ± 0.18[ab]	1.10 ± 0.02[b]	15 ± 0.86[ab]
	NaCl	72.50 ± 1.2[d]	39.66 ± 1.34[c]	28.72 ± 0.88[c]	13.50 ± 0.13[c]	0.80 ± 0.03[d]	9.0 ± 0.62[c]
	NaHS	105.0 ± 1.97[a]	57.66 ± 1.2[a]	36.39 ± 1.03[a]	19.7 ± 0.17[a]	1.20 ± 0.11[a]	16.0 ± 0.95[a]
	NaCl + NaHS	81.66 ± 1.53[c]	47.33 ± 1.4[b]	32.05 ± 1.14[b]	17.7 ± 0.15[b]	0.90 ± 0.02[c]	12.0 ± 0.79[b]

Data with different superscript letters were significantly different ($P \leq 0.05$). Data were expressed by mean values±SE (*n*=10)
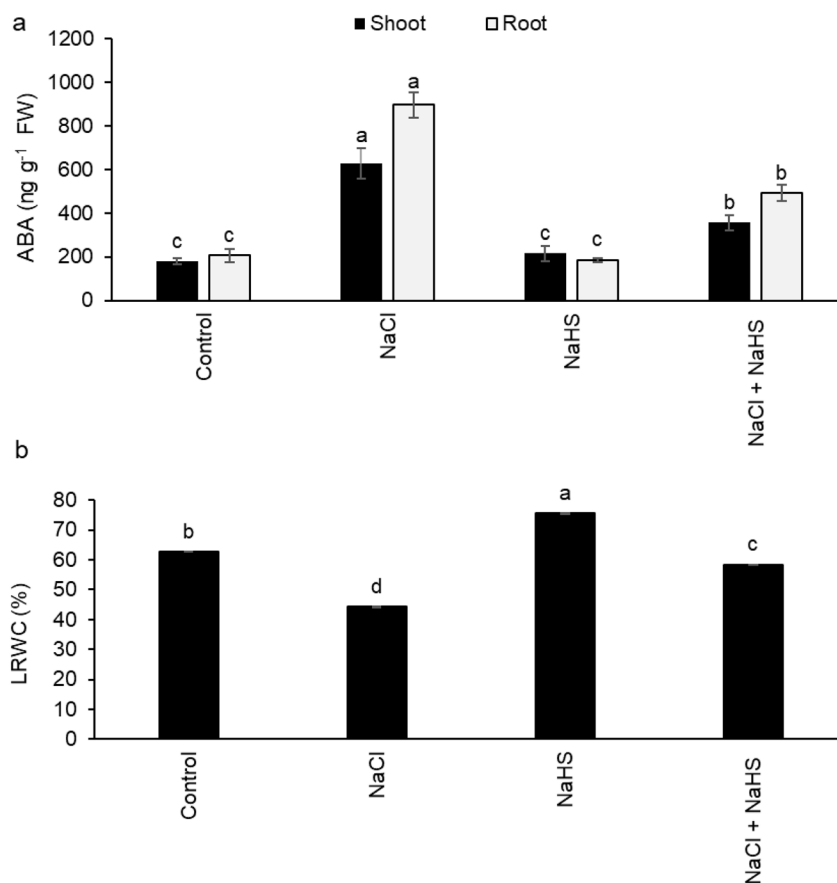
Fig. 3 Effect of NaHS pretreatment in the presence and absence of 150 mM NaCl on: (**a**) ABA content and (**b**) leaf relative water content (LRWC) of sunflower seedlings. Each value is the mean ± SD of three replicates. Bars with different letters indicate significant differences at $P \leq 0.05$

The effect of 0.5 mM H_2S priming on photosynthetic parameters in the leaves of sunflower seedlings under salinity stress is shown in Fig. 5. A significant decrease was observed in chlorophyll a, chlorophyll b, carotenoids, and total pigments under NaCl stress by 24.8%, 45%, 35%, and 31.3%, respectively, compared with the controls (Fig. 5a). H_2S priming resulted in a significant increase in the photosynthetic pigment contents when it was applied alone or in the presence of NaCl stress compared with the NaCl controls (Fig. 5a). Further, NaCl stress induced a reduction in F_v/F_m and PI_{abs} values, which were significantly restored to the control values or even higher with H_2S priming (Fig. 5b, c). Also, the expression of the Rubisco small subunit gene *HaRBCS* was downregulated by 46% in response to NaCl treatment compared with the control, while H_2S pretreatment with or without NaCl stress upregulated the expression of *HaRBCS* by 6.5 and 2.7 times, respectively, higher than that in the absence and presence of NaCl treatment (Fig. 5d). Salinity stress remarkably decreased the values of MSI in the seedling shoots and roots relative to unstressed ones; however, H_2S priming significantly increased MSI in both stressed and non-stressed conditions (Fig. 5e).

The ultrastructure of the leaf mesophyll cells of the control or H_2S-treated samples showed that all the organelles in the mesophyll cells were remarkably differentiated and well-developed (Fig. 6a, c). The cell membranes were also intact and in close contact with the cell wall, and the chloroplasts were closely arranged along the plasma membranes (Fig. 6a, c). Conversely, the fine structures of NaCl-treated leaves demonstrated partial plasmolysis in some cells, which was accompanied by a reduction in mesophyll intercellular spaces and complex vesiculation in the vacuoles and distortion of the nucleus (Fig. 6b). In addition, the number of chloroplasts decreased dramatically and showed disintegrated thylakoid membranes, and the mitochondria appeared also with dissolved cristae (Fig. 6b). On the other hand, the mesophyll cells structure under combined treatment of H_2S and 150 mM NaCl showed less deleterious symptoms of NaCl toxicity as no shrinkage of the cell membranes observed, the chloroplasts retained their membrane envelopes, as well as more orderly mitochondria and nucleus (Fig. 6d).

NaCl stress significantly reduced the content of TSS by 46.8% and 69.2% in the shoots and roots, respectively, relative to their controls, whereas H_2S priming significantly
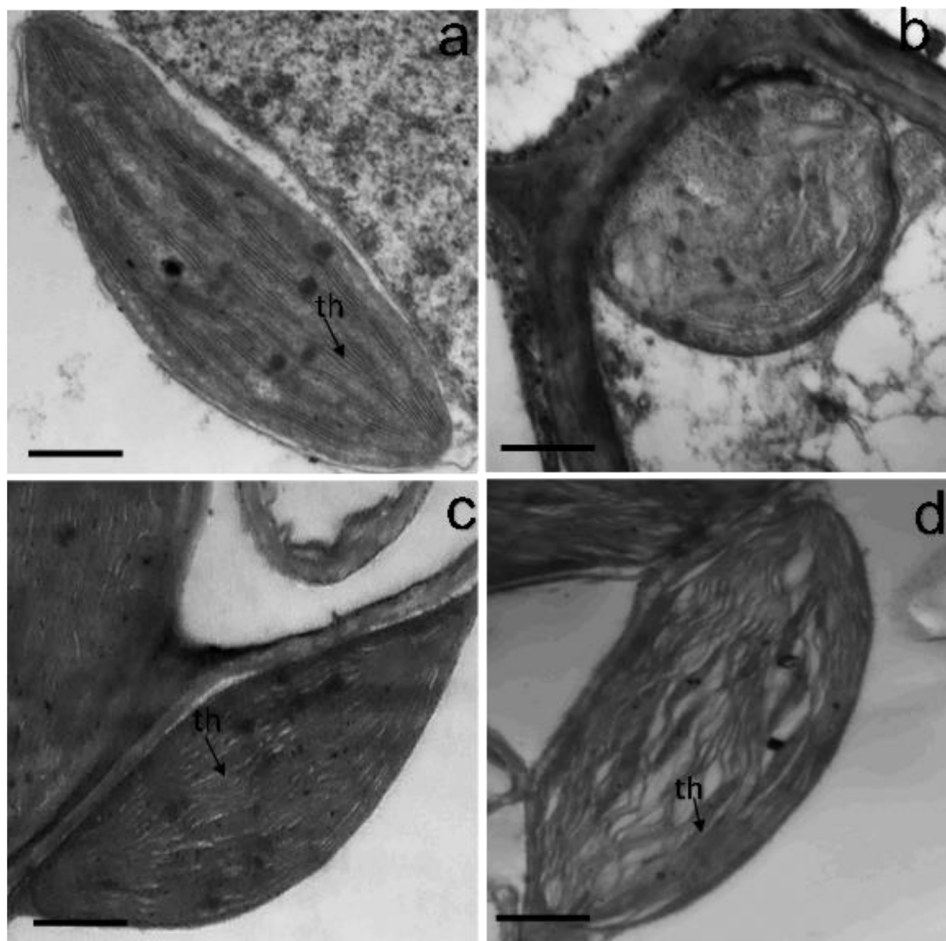
Fig. 4 Effect of NaSH pretreatment on chloroplast ultrastructure of sunflower seedlings leaves in the presence and absence of 150 mM NaCl. (**a**) control, (**b**) NaCl, (**c**) NaSH, (**d**) NaCl+NaSH. th, thylakoid membranes. Bars are 500 nm

enhanced their contents by 54.8% in the shoots and by 41.2% in the roots of salinity-stressed seedlings relative to those received NaCl treatment only (Fig. 7a). Also, NaCl treatment significantly reduced the TSP contents by 51.2% and 14.5% in the shoots and roots, respectively, relative to their controls (Fig. 7b), while H_2S priming in the presence of NaCl stress enhanced the TSP contents by 68.7% and 6.5% in the shoots and roots, respectively, compared with those of seedlings treated only with NaCl (Fig. 7b). Relative to their controls, the contents of free amino acids and proline were increased by 641.7% and 151.8% in the shoots and by 175% and 146% in the roots, respectively, in response to NaCl stress. H_2S priming significantly reduced these contents compared with the seedlings receiving only NaCl stress (Fig. 7c, d).

Discussion

Salt stress seriously affects crop growth and productivity, and changes in growth are typically the first and most noticeable responses of stressed plants. In this study, the fresh weight, dry weight, and leaf area of sunflower seedlings were significantly suppressed under NaCl stress. This salinity-induced decrease in the growth can be attributed to the osmotic action of salinity (i.e., water stress), ionic stress due to excessive ion accumulation, nutritional disequilibrium, reduced photosynthetic capacity (observed in this research), and/or oxidative stress [35–37]. However, salinity-stressed seedlings showed a marked increase in root-to-shoot dry weight ratio which might imply a higher reduction in the shoot dry weight [35] as well as an increase in root biomass production, which may favor the retention of Na^+ in the root as an adaptive response [6, 35]. We also speculate that the extensive root growth could compensate for their absorption function loss resulting from salinity treatment by dry weight accumulation [38, 39]. The reduction in growth parameters and the higher R/S ratio were also reported in different crop species in response to saline conditions [40–44]. On the other hand, the mitigative effect of H_2S on salinity-induced growth reduction most probably is interpreted as H_2S modulation of ion hemostasis, elevation of osmolyte levels (total soluble proteins and total
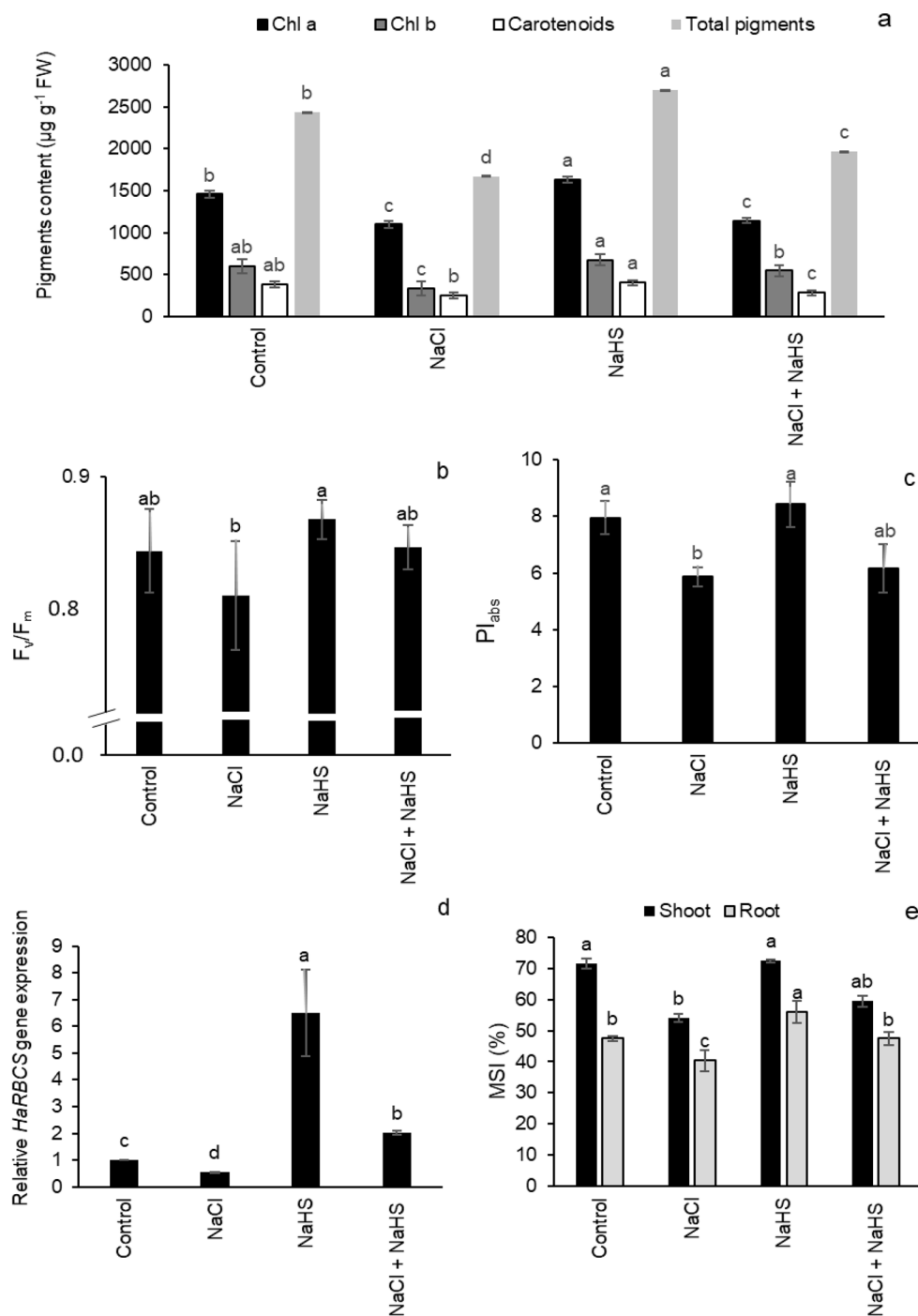
Fig. 5 Effect of NaHS pretreatment in the presence and absence of 150 mM NaCl on (**a**) photosynthetic pigment contents, (**b**) maximum efficiency of photosystem II (F_v/F_m), (**c**) performance index (PI_{abs}), (**d**) Rubisco small subunit (*HaRBCS*) gene expression, and (**e**) membrane stability index (MSI) of sunflower seedlings. Each value is the mean ± SD of three replicates. Bars with different letters indicate significant differences at $P \leq 0.05$

soluble sugars observed in this study), signaling molecule role, and scavenging of ROS under saline imposition [34, 35, 45–48]. Reduced toxic ions and elevated beneficial ones as well as ROS detoxification by H_2S priming under saline conditions have been reported as adaptive mechanisms for sunflower salinity tolerance [35]. Also, H_2S

priming followed by NaCl stress resulted in a remarkable reduction in the R/S ratio might be explained by the impact of H_2S in reducing Na^+ uptake and accumulation in both the root and shoot as previously reported by Younis and Mansour [35].
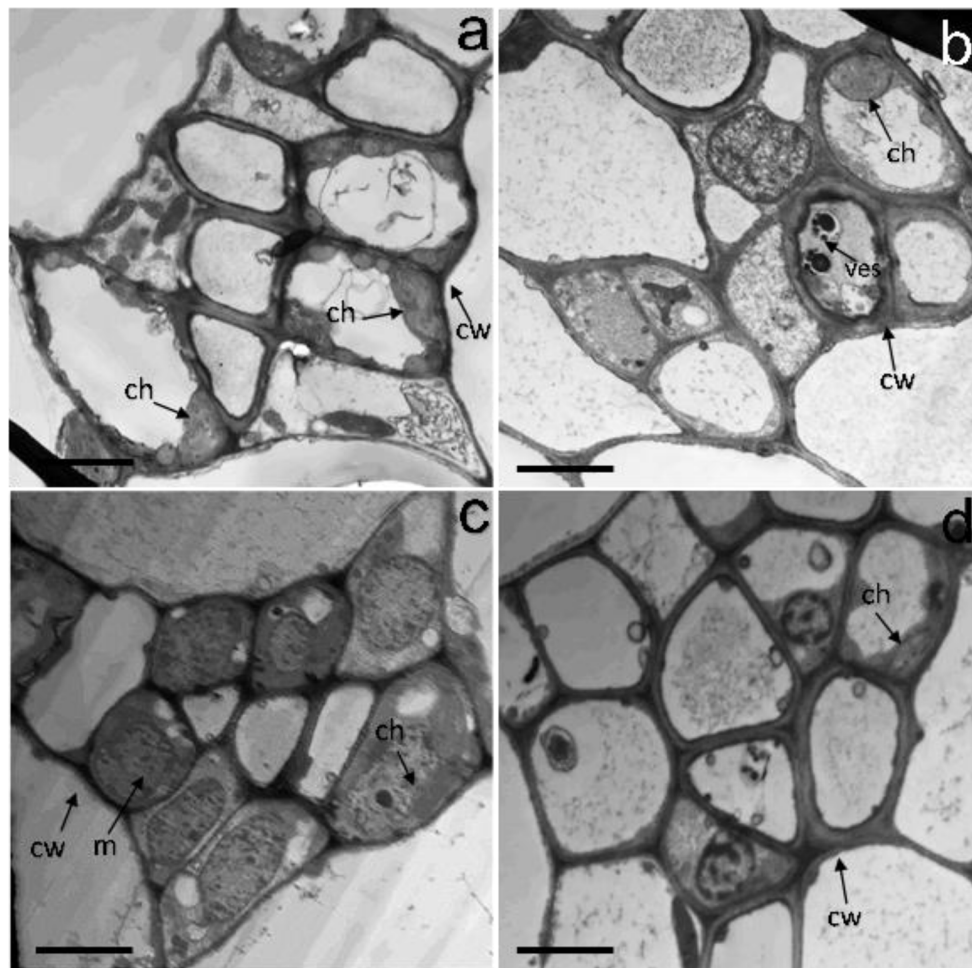
Fig. 6 Effect of NaSH pretreatment on mesophyll cells ultrastructure of sunflower seedlings leaves in the presence and absence of 150 mM NaCl. (**a**) control, (**b**) NaCl, (**c**) NaSH, (**d**) NaCl+NaSH. cw, cell wall; ch) chloroplast; m) mitochondria; and ves) vesicles. Bars are 2 μm

Stomata are important structures of photosynthetic apparatus, and gas exchange through stomata plays an important role in carbon assimilation. Therefore, abnormalities in the shapes and numbers of stomata can reduce carbon fixation capacity and ultimately disturb the photosynthetic process [49]. In the present study, NaCl treatment caused a significant reduction in stomatal index percentage, stomatal area, and opened stomata, which was accompanied by wrinkling and shrinkage of epidermal walls. These findings agreed with those of Mohamed et al. [50], De Micco et al. [51], and El-Dakak et al. [52], who reported reduced stomatal index percentage and stomatal width in different plant species under salinity stress. Additionally, many factors regulate stomatal mechanics, including ABA, NO, specific ions, and water channels [53, 54]. It has also been shown that ABA accumulation is a cell signaling process in response to salinity stress to help plants survive by inhibiting stomatal opening, transpiration, and plant expansion [53]. In the current work, salinity-induced stomatal closure in leaves of sunflower plants was associated with ABA accumulation and reduced LRWC, which is in accordance with the results of Gupta et al. [55], Gupta and Seth [56], and Niu et al. [54] who demonstrated salinity-induced ABA production was involved in the regulation of stomatal closure to regulate plant internal water balance. However, H_2S priming improved stomatal opening which was associated with lower ABA content. Our finding is consistent with the results of Lisjak et al. [57, 58], who report H_2S promotion of stomata to open by reducing ABA accumulation in *Arabidopsis thaliana*. We also propose that stomatal aperture enhancement by H_2S may increase CO_2 availability in the mesophyll cells as well as water homeostasis, and thereby stimulate the photosynthesis efficiency observed in this study [30, 34, 45, 59].

Salinity stress affects photosynthesis by perturbing chloroplasts' ultrastructure and synthesis of pigments [60]. Chloroplasts play a central role in photosynthesis, serving as the primary site for energy conversion and the assimilation of power production [20, 21]. In
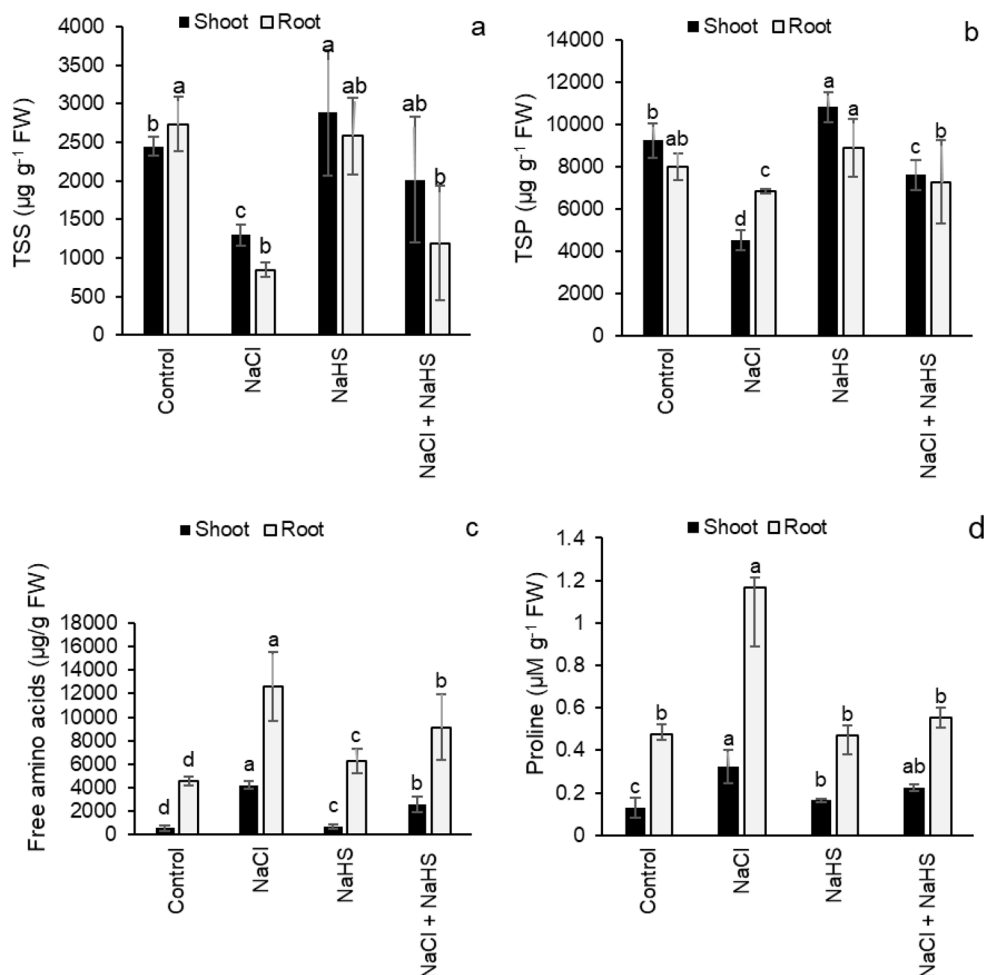
Fig. 7 Effect of NaHS pretreatment in the presence and absence of 150 mM NaCl on (**a**) total soluble sugar (TSS) content, (**b**) total soluble protein (TSP) content, (**c**) free amino acids content, and (**d**) proline content of sunflower seedlings. Each value is the mean ± SD of three replicates. Bars with different letters indicate significant differences at $P \leq 0.05$

the current research, the ultrastructure of the chloroplasts was greatly altered under salinity stress showing distorted thylakoid and an unrecognizable grana structure, which might be brought about by salinity-induced oxidative damage [18, 61, 62] and disturbed ion balance in the chloroplasts [63]. Similar impacts of salinity stress on the chloroplast structure were observed in cucumber [64], Arabidopsis [65], potato [66], rice [67], eggplant [17], and faba bean [52]. NaCl stress also caused a significant reduction in photosynthetic pigments (chlorophylls and carotenoids): chlorophyll decline might be due to the inhibition of chlorophyll synthesis due to salinity-reduced levels of iron and magnesium, enhanced activity of chlorophyllase by Na^+ and Cl^- accumulation, and/or photoinhibition or ROS toxicity [18, 68]. The distortion of thylakoid membranes may also lead to chlorophyll loss, as Chuartzman et al. [69] reported. NaCl-induced decline in the carotenoid content could be attributed to the inhibition of carotenoid biosynthesis enzymes' activity and the downregulation of their transcription levels

[70]. Additionally, the decreased value of photosynthetic performance (PI_{abs}) and the maximal photochemical efficiency of PSII (F_v/F_m) in salinity-stressed sunflower leaves are indicative of the photoinhibition caused by NaCl on the donor side of the PSII [62]. Also, the disappearance of grana observed in this study may cause a reduction in F_m and F_v/F_m leading to the downregulation of PSII activity [18, 71]. H_2S priming, however, enhanced photosynthetic pigment content and preserved chloroplast ultrastructure, suggestive of H_2S role as a signaling molecule stimulating the chloroplast biogenesis and increasing the quantity of grana lamellae [72], repairing the biomembrane [34], enhancing the antioxidants, and lowering Na^+ uptake and translocation [35], which ultimately protected the thylakoid membranes and boosted the photosynthetic capacity of NaCl-challenged sunflower plants. Similarly, other published works reported H_2S promotion of chlorophyll contents and photosynthetic capacity in a variety of plants [73–75]. In the same trend, H_2S-triggered carotenoid concentration can be explained by the

contention that H_2S upregulated the expression levels of the carotenoid-related genes and thus their biosynthesis enzyme activities [70] as well as enhancing osmoregulators under stress [34]. It is noteworthy that Zhao et al. [70] showed the carotenoid accumulation increase was associated with improved salinity tolerance in carrots as the carotenoids are essential components of the photosynthetic antenna and reaction center complexes, as precursors in signaling pathways, responsible for antioxidant defense, and other protective roles that help plants cope with abiotic stress. Further, H_2S showed effective recovery potential in enhancing electron transport efficiency and photochemical activity of PSII as reflected by higher F_v/F_m and PI_{abs} values. This H_2S beneficial effect has also been shown in various crops under stressful conditions [59, 76–78]; altogether reporting that H_2S plays a key role in activating plant photosynthesis machinery possibly by increasing Mn ion and extrinsic proteins of oxygen-evolving complex, that further improved the electron donation from water to PSII or might have caused the conformational changes in D1 protein, thereby altering the properties of PSII electron acceptor that ultimately improved the PSII activity.

The application of H_2S elevated the expression level of the small subunit *HaRBCS* gene, which most likely activated ribulose-1,5-bisphosphate carboxylase (Rubisco) and thus enhanced the photosynthesis rate; the finding was reported by other researchers [79, 80]. The Rubisco small subunit is indicated to be a potential engineering target to improve the performance of Rubisco [19], and based on our findings, we recommend it for engineering biology approaches to modulate Rubisco catalysis activating the photosynthesis and hence crop performance under saline conditions. In addition, the accumulation of different osmolytes (soluble sugars, soluble proteins, and carotenoids) in the sunflower seedlings in response to H_2S priming in the current study, is suggestive of their role in protecting the architecture and functions of the chloroplast membranes, enzymes, and other cell structures against ROS damage and the toxicity of greater concentrations of intracellular toxic ions, as well as acting as osmotic regulators [18, 34, 81–84], which resulted in enhanced photosynthesis, stabilized subcellular structures, and osmotic adjustment, and ultimately the adaptability of sunflower seedlings to NaCl stress. Moreover, NaCl-enhanced burst of proline in sunflower seedlings (more so in roots) might be associated with salinity-induced ABA content observed in this research as ABA has been reported to elevate proline production in various stressed plants under saline conditions [85, 86]. Greater proline, and possibly other free amino acids, in roots relative to shoots observed in this work is most likely attributed to proline higher biosynthesis and active expression of proline transporters reported in roots than

in shoots under stress conditions [87]. Salinity-induced proline accumulation was significantly reduced by H_2S priming, which was previously found by other investigators in crop plants under salinity stress [45, 83, 88, 89]. It seems that the beneficial proline functions in response to saline stress were compensated by the accumulation of other organic osmolytes observed in the current research including soluble sugars, soluble proteins, and carotenoids under H_2S priming.

The TEM results of the mesophyll cells under NaCl stress showed disorganization of the protoplast which is possibly caused by salinity-induced osmotic stress [90]. Additionally, thickened cell walls, partial plasmolysis, and decreased intercellular spaces under salinity treatment imply water loss from the cells triggered by Na^+ and Cl^- accumulation in the apoplast [66]. Further, the observed vesicles under salinity treatment are most probably interpreted by the sequestration of Na^+ and Cl^- into the vacuoles as well as by membrane system damage induced by ROS toxicity forming small vacuolations [66, 91]. Also, salinity inhibits the absorption of Ca^{2+}, further leading to instability of the cell membranes and cell walls, which might cause such cellular aberrations [35]. The H_2S priming alleviated these cellular aberrations of the mesophyll cells by H_2S role in biomembrane repairing [34], ROS scavenging, Na^+, and Cl^- uptake restriction as well as K^+ and Ca^{2+} content elevation [35], resulting in membrane integrity and osmotic balance maintenance reflected in the elevated value of MSI found in this work. Alamer [84] also reported a similar alleviating impact on the MSI by H_2S supply under salinity stress in wheat.

Conclusion

As maintaining the structural and functional organization of chloroplasts is vital for the dynamics and flexibility of the photosynthetic apparatus, H_2S priming effectively modulated the photosynthetic machinery of sunflower under salinity stress as evidenced by stomatal (density and aperture) and non-stomatal (F_v/F_m, FI_{abs}, Rubisco small subunit overexpression, photosynthetic pigment elevation, and organic osmolyte accumulation) effectors, which implied the potential use of the priming strategy with H_2S to increase the photosynthetic performance and efficiency and to preserve the chloroplast structure thereby enhancing sunflower tolerance and expectedly its productivity under saline conditions.

Materials and methods

Plant growth conditions and stress imposition

Sunflower (*Helianthus annuus* L.) seeds of cultivar 'Sakha 53' were obtained from the Agricultural Research Center, Giza, Egypt, and kept in the dark at 4 °C. The seeds were surface sterilized by immersion in 1% (w/v) sodium hypochlorite solution for 10 min and then rinsed thoroughly

with distilled water. The sterilized sunflower seeds were divided into two groups: the first group was primed with distilled water (control), and the second one was primed with NaHS (Sigma-Aldrich, USA) as the exogenous H_2S donor at a concentration of 0.5 mM at room temperature (25 ± 2 °C). Both control and H_2S-treated seeds were kept in their respective medium for 2 h. The H_2S concentration (0.5 mM) was adopted based on our previous work [35] that performed under the same growth conditions and exhibited the best results in improving sunflower salinity tolerance. The seeds were then dried on filter paper for approximately 24 h before germination. The seeds were then sown in plastic pots (diameter 15 cm, height 30 cm) containing 1.5 Kg of sieved air-dried clay soil and peat moss (peat moss: clay, 1:1 v/v). The experiment was conducted using a completely randomized design in a controlled growth chamber (model V3-DM, Vision Scientific Company, Daejeon-Si, South Korea) which was maintained at 27/18°C Day/night temperatures, a 50% relative humidity, a photosynthetic photon flux density (PPFD) of 400 µmol m^{-2} s^1, and a 14-h photoperiod. NaHS-pretreated and non-pretreated seeds were irrigated with tape water until seedling establishment for 14 d, and then they were exposed to two levels of NaCl (0 and 150 mM) in three replications for 7 d. Each replication was composed of 10 plants. The following treatments of sunflower seedlings were therefore established: (1) control, untreated and irrigated with tape water; (2) NaCl stress, untreated and irrigated with 150 mM NaCl solution; (3) NaHS, NaHS-priming and irrigated with tape water; and (4) NaHS+NaCl, NaHS-priming and irrigated with 150 mM NaCl solution. Twenty-one-day-old seedlings were harvested and five plants per treatment were subjected to measuring growth parameters. Fresh leaves for photosynthetic and microscopic studies were taken as described below, while others were rapidly frozen in liquid nitrogen and stored at -80 °C for other physiological and biochemical analyses.

Determination of growth parameters

Using a ruler, the plant height (cm) was measured as the distance between the terminal bud and the maximal extremity of the pivoting root. Seedlings were immediately weighed to determine their fresh weight (FW, g per seedling), then dried at 60 °C for 96 h to obtain the dry weight (DW, g per seedling) using a balance (TWIII, USA). Root/shoot ratio (R/S) was obtained through the relation:

$$\mathrm{R/S\ ratio} = \mathrm{RDW}/(\mathrm{LDW}+\mathrm{SDW})$$

where RDW is root dry weight, LDW is leaf dry weight, and SDW is stem dry weight. Leaf area (cm^2) was obtained by the equation:

$$\mathrm{Leaf\ area\ (cm^2)} = x/y$$

where x is the weight (g) of the area covered by the leaf outline on a millimeter graph paper, and y is the weight of one cm^2 of the same graph paper.

Stomatal measurements

For stomatal measurements, the first pair of fully expanded leaves were used. A strip of the upper and lower epidermis from the middle portion of the leaf was peeled off and mounted in glycerol after staining with safranin. Stomatal density (the number of stomata per square millimeter of leaf surface) and sizes were recorded at 400 magnifications under the microscope (Optica, Italy) coupled to a clear camera (digital premiere MA88-900, Italy) and submitted to the Image J Analyzer. The area of the stomata was calculated by multiplying its length by width and then with 0.785; a common factor meant for elliptical structure [92]. The stomatal index was calculated as a percent (%) according to Rengifo et al. [93] using the equation:

$$\mathrm{Stomatal\ Index(\%)} = \begin{array}{l}\mathrm{number\ of\ stomata}/(\mathrm{number\ of\ stomata}\\+\mathrm{number\ of\ epidermal\ cells}) \times 100\end{array}$$

The presented data were the mean$\pm$SE of measurements of 10 different fields of view of the leaves' upper (adaxial) and lower (abaxial) surfaces from 10 individual plants.

Transmission electron microscopy (TEM)

TEM was performed as described previously by Cao et al. [94]. Samples (1 cm^2) from the middle of the second flag leaves were collected, then sliced, and fixed immediately in 4% glutaraldehyde in 100 mM sodium cacodylate buffer at pH 7.2 overnight. Following glutaraldehyde fixation, samples were post-fixed in 2% osmium tetroxide in the same cacodylate buffer, stained in 1% aqueous uranyl acetate for 8 h, dehydrated in acetone, and embedded in Spurr's resin [95]. Ultrathin Sect. (300 nm) of the samples were then examined under transmission electron microscope (TEM; JEM 1011, JEOL, Tokyo, Japan) at 80 kV, and photographed for image analysis with an AMT digital image capture system.

Measurement of photosynthetic parameters

A portable fluorometer (Handy PEA, Hansatech, Norfolk, UK) was used to determine the photosynthetic performance (PI_{abs}) and the maximal quantum yield of PSII photochemistry (F_v/F_m) as described by Maxwell and Johnson [22]. Chlorophyll a (Chl a), chlorophyll b (Chl b), and carotenoids (Car) were extracted in 80% (v/v) acetone and measured by UV spectrophotometer UNICAM Helios α (Unicam, Cambridge, UK) according to Metzner et al. [96]. The pigment concentration was calculated and

expressed in μg g^{-1} FW, and then total pigment contents were calculated.

Determination of total soluble sugars (TSS)

Total soluble sugar concentration was measured according to the method described by Xu et al. [97]. Fresh leaves (0.5 g) were ground with a pestle in an icy mortar, and mixed with 5 mL of distilled water, immediately followed by incubating in boiling water for 30 min. After centrifugation at 4,000 × g for 5 min and removal of the supernatant, the pellet was resuspended and reextracted twice. Three supernatants were transferred to a 25-mL volumetric flask and distilled water was added to make up the volume. Afterward, 1 mL of sample extract was added to 3 mL of anthrone reagent and mixed well. After heating the sample at 100 °C for 10 min and cooling down, the TSS content was measured at the absorbance of 620 nm (Spectronic 601, Milton Roy Company, Texas, USA).

Determination of total soluble proteins

Total soluble protein contents in leaves were determined using a modified method of Bradford [98]. Fresh samples (1 g) were ground in liquid nitrogen and homogenized in Tris-HCl (100 mM, pH 8.0) extraction buffer containing EDTA (1 mM), DTT (5 mM), Triton X-100 (0.02%, v/v), and glycerol (10%, v/v). The resulting homogenates were centrifuged at 17,000×g for 20 min at 4 °C. One mL of sample extract was added to 5 mL of 0.01% (w/v) Coomassie Brilliant Blue G-250 containing 4.7% (w/v) ethanol and 8.5% (w/v) phosphoric acid and mixed well. After incubation at room temperature for 2 min, the absorbance was recorded at 595 nm (Spectronic 601, Milton Roy Company, Texas, USA).

Determination of total free amino acids

One gram of fresh tissue was ground thoroughly with 20 mL of distilled water. The mixture was then quantitatively transferred to a boiling tube, and maintained at 80 °C for 15 min. The insoluble residue was removed by filtration and the filtrate was made up to a certain volume and used for the estimation of total free amino acids photometrically with the ninhydrin method of Muting and Kaiser [99].

Determination of proline content

Extraction of proline was performed according to the method of Carillo and Gibbon [100]. The cold extraction process was used by mixing plant material (0.5 g) with a combination of ethanol: water (40:60 v/v). The supernatant was collected after the mixture was left overnight at 4 °C. Proline was quantified by reading absorbance at 520 nm (Spectronic 601, Milton Roy Company, Texas, USA) and using L-proline as the standard.

Determination of ABA content

ABA was extracted using freshly collected samples according to the method described by Almeida Trapp et al. [101]. The liquid nitrogen-grinded samples (5 g) were shaken for 30 min and centrifuged at 16,000 x g and 4 °C for 5 min. The supernatant was transferred into a new micro-centrifuge tube and dried in speed vac. After drying, 100 μl of MeOH was added to each sample, which was then mixed with a vortex and centrifuged at 16,000 x g and 4 °C for 10 min. The quantity of ABA was determined using high-performance liquid chromatography (HPLC; instrument E-Chrom Tech, LC 1620, USA). The samples were assayed against ABA as internal standards.

Leaf relative water content determination

The relative water content of plant leaves (LRWC) was measured by the method of Pan et al. [102]. Leaves from selected plants were detached and weighed to obtain their fresh weight (FW), and then soaked in distilled water at room temperature for 24 h, weighed to obtain turgid weight (TW), and then dried in an oven at 80 °C for 48 h to have a constant dry weight (DW). The LRWC was then calculated using the following formula:

$$\text{LRWC}\,(\%) = (FW - \text{DW})/(\text{TW} - \text{DW}) \times 100$$

Membrane stability index (MSI) determination

The MSI was determined according to Sairam et al. [103]. Leaf samples (200 mg) were immersed in 10 mL of deionized water and divided into 2 sets. One set was kept at 40 °C for 30 min and its conductivity was recorded (C1) using a conductivity meter (HI 8733, Hanna Instruments, Woonsocket, RI, USA). The second set was kept in a boiling water bath (100 °C) for 15 min and its conductivity was also recorded (C2). The MSI was calculated as:

$$\text{MSI} = [1 - (\text{C1}/\text{C2})] \times 100$$

RNA extraction and quantitative real-time PCR (qRT-PCR)

Total RNA was extracted from 30 mg of fresh leaves of each treatment using a Gene JET™ RNA purification Kit (Thermo Fisher Scientific, MA, USA). One μg of total RNA was reverse transcribed into cDNA using the Revert Aid First Strand cDNA Synthesis Kit (Thermo Fisher Scientific, MA, USA). Ribulose-1,5-bisphosphate carboxylase (Rubisco) small subunit *RBCS* gene sequence was previously searched in the National Center for Biotechnology Information (NCBI, www.ncbi.nlm.nih.gov) to design gene-specific primers for qRT-PCR. Primer sequences for the reactions were *HARBCS1*; Y00431 FP: 5′- CATTTGACACGTGGCTCTCC −3′; RP: 5′- A GGATGTTGTGGCTCTTGGA −3 and for AAF82805

(ACTIN sequence from sunflower) FP: 5′-AGGGCGG TCTTTCCAAGTAT −3; RP: 5′-ACATACATGGCGG GAACATT −3. PCR amplification specificity was verified using melting curve analysis and data were analyzed using the $2^{-\Delta\Delta Ct}$ method [104] after normalized to the expression of each ACTIN gene.

Statistical analysis

The results were subjected to a one-way analysis of variance (ANOVA) using the software package SPSS 25.0 (IBM, Corp, Armonk, NY, USA). The comparison of the means of different treatments was carried out using Duncan's multiple range test at a significant level of 5% ($P\leq0.05$). All experimental data are expressed as means±standard deviation (SD) of three replications.

Declarations

References
1. Mujeeb-Kazi A, Munns R, Rasheed A, Ogbonnaya FC, Ali N, Hollington P. Breeding strategies for structuring salinity tolerance in wheat. Adv Agron. 2019;155:121–87.
2. Da Silva CJ, Fontes EPB, Modolo LV. Salinity-induced accumulation of endogenous H₂S and NO is associated with modulation of the antioxidant and redox defense systems in *Nicotiana tabacum* L. Cv. Havana Plant Sci. 2017;256:148–59.
3. Reddy INBL, Kim B-K, Yoon I-S, Kim K-H, Kwon T-R. Salt tolerance in rice: focus on mechanisms and approaches. Rice Sci. 2017;24:123–44.
4. FAO. FAO Global Soil Partnership (Soil salinity). 2020.
5. Karle SB, Guru A, Dwivedi P, Kumar K. Insights into the role of gasotransmitters mediating salt stress responses in plants. J Plant Growth Regul. 2021;40:2259–75.
6. Acosta-Motos JR, Ortuño MF, Bernal-Vicente A, Diaz-Vivancos P, Sanchez-Blanco MJ, Hernandez JA. Plant responses to salt stress: adaptive mechanisms. Agronomy. 2017;7:18.
7. Arif Y, Singh P, Siddiqui H. Salinity induced physiological and biochemical changes in plants: an omic approach towards salt stress tolerance. Plant Physiol Biochem. 2020;156:64–77.
8. dos Santos TB, Ribas AF, de Souza SGH. Physiological responses to drought, salinity, and heat stress in plants: a review. Stresses. 2022;2:113–35.
9. Mansour MMF, Salama KHA. Proline and abiotic stresses: responses and adaptation. In: Hasanuzzaman M, editor. Plant Ecophysiology and Adaptation under Climate Change: mechanisms and perspectives II, mechanisms of adaptation and stress amelioration. Singapore: Springer; 2020. pp. 357–97.
10. Xu J, Xu Y, Wang Y, Lv Z, Liu X, Sun W. Exogenous salicylic acid improves photosynthetic and antioxidant capacities and alleviates adverse effects of cherry rootstocks under salt stress. J Plant Growth Regul. 2024. https://doi.org/10.1007/s00344-023-11195-6.
11. Sarabi B, Fresneau C, Ghaderi N, Bolandnazar S, Streb P, Badeck F-W. Stomatal and non-stomatal limitations are responsible in down-regulation of photosynthesis in melon plants grown under the saline condition: application of carbon isotope discrimination as a reliable proxy. Plant Physiol Biochem. 2019;141:1–19.
12. Hnilickova H, Kraus K, Vachova P, Hnilicka F. Salinity stress affects photosynthesis, malondialdehyde formation, and proline content in Portulaca oleracea L. Plants. 2021;10:845.
13. Zhang Y, Zhou X, Dong Y, Zhang F, He Q, Chen J. Seed priming with melatonin improves salt tolerance in cotton through regulating photosynthesis, scavenging reactive oxygen species and coordinating with phytohormone signal pathways. Ind Crops Prod. 2021;169:113671.
14. Zeeshan M, Lu M, Sehar S, Holford P, Wu F. Comparison of biochemical, anatomical, morphological, and physiological responses to salinity stress in wheat and barley genotypes deferring in salinity tolerance. Agronomy. 2020;10:127.
15. Oláh V, Hepp A, Irfan M, Mészáros I. Chlorophyll fluorescence imaging-based duckweed phenotyping to assess acute phytotoxic effects. Plants. 2021;10:2763.
16. Oikonomou A, Ladikou E, Papadakis I, Sotiras M-I, Landi M. Salinity alters plant's allometry and sugar metabolism, and impairs the photosynthetic process and photosystem II efficiency in *Eriobotrya japonica* plants. Agrochimica. 2019;63:27–42.
17. Alkhatib R, Abdo N, Mheidat M. Photosynthetic and ultrastructural properties of eggplant (Solanum melongena) under salinity stress. Horticulturae. 2021;7:181.
18. Masarmi AG, Solouki M, Fakheri B, Kalaji HM, Mahgdingad N, Golkari S. Comparing the salinity tolerance of twenty different wheat genotypes on the basis of their physiological and biochemical parameters under NaCl stress. PLoS ONE. 2023;18:e0282606.
19. Mao Y, Catherall E, Díaz-Ramos A, Greiff GRL, Azinas S, Gunn L. The small subunit of Rubisco and its potential as an engineering target. J Exp Bot. 2023;74:543–61.
20. Teng J, Liao P, Wang M. The role of emerging micro-scale vegetables in human diet and health benefits—An updated review based on microgreens. Food Funct. 2021;12:1914–32.
21. Stefanov MA, Rashkov GD, Apostolova EL. Assessment of the photosynthetic apparatus functions by chlorophyll fluorescence and P700 absorbance in C3 and C4 plants under physiological conditions and under salt stress. Int J Mol Sci. 2022;23:3768.
22. Maxwell K, Johnson GN. Chlorophyll fluorescence—a practical guide. J Exp Bot. 2000;51:659–68.
23. de Castro C, de Leite R. Main aspects of sunflower production in Brazil. Oilseeds Fats Crops Lipids. 2018;25:D104.
24. Miladinović D, Hladni N, Radanović A, Jocić S, Cvejić S. Sunflower and climate change: possibilities of adaptation through breeding and genomic selection. In: Kole C, editor. Genomic Designing of Climate-Smart Oilseed Crop. Cham: Springer; 2019. pp. 173–238.
25. de Oliveira Filho JG, Egea MB. Sunflower seed byproduct and its fractions for food application: an attempt to improve the sustainability of the oil process. J Food Sci. 2021;86:1497–510.
26. El-Hamidi M, Zaher FA. Production of vegetable oils in the world and in Egypt: an overview. Bull Natl Res Cent. 2018;42:1–9.
27. Mansour MMF, Ali EF, Salama KHA. Does seed priming play a role in regulating reactive oxygen species under saline conditions? In: Hasanuzzaman M, Fotopoulos V, Nahar K, Fujita M, editors. Reactive oxygen, Nitrogen, and Sulfur species in plants: production metabolism, signaling, and Defense mechanisms. London: Wiley; 2019. pp. 437–85.

28. Zulfiqar F, Hancock JT. Hydrogen sulfide in horticulture: emerging roles in the era of climate change. Plant Physiol Biochem. 2020;155:667–75.

29. Pagano A, Macovei A, Xia X, Padula G, Hołubowicz R, Balestrazzi A. Seed priming applied to onion-like crops: state of the art and open questions. Agronomy. 2023;13:288.

30. Duan B, Ma Y, Jiang M, Yang F, Ni L, Lu W. Improvement of photosynthesis in rice (*Oryza sativa* L.) as a result of an increase in stomatal aperture and density by exogenous hydrogen sulfide treatment. Plant Growth Regul. 2015;75:33–44.

31. Jiang J, Ren X, Li L, Hou R, Sun W, Jiao C. H$_2$S regulation of metabolism in cucumber in response to salt-stress through transcriptome and proteome analysis. Front Plant Sci. 2020;11:1283.

32. Goyal V, Jhanghel D, Mehrotra S. Emerging warriors against salinity in plants: nitric oxide and hydrogen sulfide. Physiol Plant. 2021;171:896–908.

33. Fang H, Liu R, Yu Z, Shao Y, Wu G, Pei Y. Gasotransmitter H$_2$S accelerates seed germination via activating AOX mediated cyanide-resistant respiration pathway. Plant Physiol Biochem. 2022;190:193–202.

34. Li Z-G, Fang J-R, Bai S-J. Hydrogen sulfide signaling in plant response to temperature stress. Front Plant Sci. 2024;15:1337250.

35. Younis AA, Mansour MMF. Hydrogen sulfide priming enhanced salinity tolerance in sunflower by modulating ion hemostasis, cellular redox balance, and gene expression. BMC Plant Biol. 2023;23:525.

36. AbdElgawad H, Zinta G, Hegab MM, Pandey R, Asard H, Abuelsoud W. High salinity induces different oxidative stress and antioxidant responses in maize seedlings organs. Front Plant Sci. 2016;7:276.

37. Olmo A, Garcia-Sanchez F, Simon I, Lidon V, Alfosea-Simon M, Camara-Zapata J. Characterization of the ecophysiological responses of three pomegranate cultivars to salinity. Photosynthetica. 2019;571015–1024.

38. Wang SF, Hu Y, Li Z, Sun H, Chen Y. Effects of NaCl stress on growth and mineral ion uptake, transportation and distribution of Quercus virginiana. Acta Ecol Sin. 2010;30:4609–16.

39. Abideen Z, Koyro H-W, Huchzermeyer B, Ahmed MZ, Gul B, Khan MA. Moderate salinity stimulates growth and photosynthesis of Phragmites karka by water relations and tissue specific ion regulation. Environ Exp Bot. 2014;105:70–6.

40. Zafar Z, Rasheed F, Shaheen F, Hussain Z, Anwaar AH, Rizwan M. The influence of salt stress on growth and biomass production of Populus deltoides. Int J Biosci. 2018;13:191–7.

41. Liu Z, Zhu J, Yang X, Wu H, Wei Q, Wei H. Growth performance, organ-level ionic relations and organic osmoregulation of Elaeagnus angustifolia in response to salt stress. PLoS ONE. 2018;13:e0191552.

42. Rasheed F, Bakhsh R, Qadir I. Trade-off between shoot and root dry weight along with a steady CO2 assimilation rate ensures the survival of Eucalyptus camaldulensis under salt stress. J Sci. 2020;66:452–60.

43. Shalaby OAE-S, Farag R, Ibrahim MFM. Effect of hydrogen sulfide and hydrogen peroxide on growth, yield and nutrient content of broccoli plants grown under saline conditions. Sci Hortic. 2023;316:112035.

44. Zuo G, Huo J, Yang X, Mei W, Zhang R, Khan A. Photosynthetic mechanisms underlying NaCl-induced salinity tolerance in rice (*Oryza sativa*). BMC Plant Biol. 2024;24:1–10.

45. Ekinci M, Yildirim E, Turan M. Ameliorating effects of hydrogen sulfide on growth, physiological and biochemical characteristics of eggplant seedlings under salt stress. South Afri J Bot. 2021;143:79–89.

46. Liu H, Wang J, Liu J, Liu T, Xue S. Hydrogen sulfide (H$_2$S) signaling in plant development and stress responses. aBIOTECH. 2021;2:32–63.

47. Dawood MFA, Zaid A, Latef AAHA. Salicylic acid spraying-Induced Resilience Strategies against the Damaging impacts of Drought and/or salinity stress in two varieties of *Vicia faba* L. Seedlings. J Plant Growth Regul. 2022;41:1919–42.

48. Yildirim E, Ekinci M, Turan M, Ors S, Dursun A. Physiological, morphological and biochemical responses of exogenous hydrogen sulfide in salt-stressed tomato seedlings. Sustainability. 2023;15:1098.

49. Farooq M, Hussain M, Wakeel A, Siddique KHM. Salt stress in maize: effects, resistance mechanisms, and management. A review. Agron Sustain Dev. 2015;35:461–81.

50. Mohamed IAA, Shalby N, Bai C, Qin M, Agami RA, Jie K, et al. Stomatal and photosynthetic traits are associated with investigating sodium chloride tolerance of Brassica napus L. cultivars. Plants. 2020;9:62.

51. De Micco V, Arena C, Amitrano C, Rouphael Y, De Pascale S, Cirillo C. Changes in morpho-anatomical and eco-physiological responses of Viburnum tinus l. var lucidum as modulated by sodium chloride and calcium chloride salinization. Horticulturae. 2022;8:119.

52. El-Dakak RA, Badr RH, Zeineldein MH, Swedan EA, Batrawy O, El, Hassaballah AF. Effect of chilling and salinity stress on photosynthetic performance and ultrastructure of chloroplast in faba beans (*Vicia faba* L.) leaves. Rend Lincei Sci Fis Nat. 2023;34:1–10.

53. Waśkiewicz A, Beszterda M, Goliński P. ABA: role in plant signaling under salt stress. In: Ahmad P, Azooz MM, Prasad MNV, editors. Salt stress in plants: Signalling, Omic, and adaptation. New York: Springer; 2013. pp. 175–96.

54. Niu M, Xie J, Chen C, Cao H, Sun J, Kong Q. An early ABA-induced stomatal closure, Na$^+$ sequestration in leaf vein and K$^+$ retention in mesophyll confer salt tissue tolerance in Cucurbita species. J Exp Bot. 2018;69:4945–60.

55. Gupta P, Srivastava S, Seth CS. 24-Epibrassinolide and sodium nitroprusside alleviate the salinity stress in *Brassica juncea* L. Cv. Varuna through cross-talk among proline, nitrogen metabolism and abscisic acid. Plant Soil. 2017;411:483–4898.

56. Gupta P, Seth CS. Interactive role of exogenous 24 Epibrassinolide and endogenous NO in *Brassica juncea* L. under salinity stress: evidence for NR-dependent NO biosynthesis. Nitric Oxide. 2020;97:33–47.

57. Lisjak M, Srivastava N, Teklic T, Civale L, Lewandowski K, Wilson I. A novel hydrogen sulfide donor causes stomatal opening and reduces nitric oxide accumulation. Plant Physiol Biochem. 2010;48:931–5.

58. Lisjak M, Teklić T, Wilson ID, Wood M, Whiteman M, Hancock JT. Hydrogen sulfide effects on stomatal apertures. Plant Signal Behav. 2011;6:1444–56.

59. Jiang JL, Tian Y, Li L, Yu M, Hou RP, Ren XM. H$_2$S alleviates salinity stress in cucumber by maintaining the Na$^+$/K$^+$ balance and regulating H$_2$S metabolism and oxidative stress response. Front Plant Sci. 2019;10:678.

60. Ashraf M, Harris PJC. Photosynthesis under stressful environments: an overview. Photosynthetica. 2013;51:163–90.

61. Mohamed HI, Abd-El Hameed AG. Molecular and biochemical markers of some *Vicia faba* L. genotypes in response to storage insect pests infestation. J Plant Interact. 2014;9:618–26.

62. Taïbi K, Taïbi F, Abderrahim LA, Ennajah A, Belkhodja M, Mulet JM. Effect of salt stress on growth, chlorophyll content, lipid peroxidation and antioxidant defence systems in *Phaseolus vulgaris* L. South Afri J Bot. 2016;105:306–12.

63. Salama S, Trivedi S, Busheva M, Arafa AA, Garab G, Erdei L. Effects of NaCl salinity on growth, cation accumulation, chloroplast structure and function in wheat cultivars differing in salt tolerance. J Plant Physiol. 1994;144:241–7.

64. Shu S, Guo S, Sun J, Yuan L. Effects of salt stress on the structure and function of the photosynthetic apparatus in Cucumis sativus and its protection by exogenous putrescine. Physiol Plant. 2012;146:285–96.

65. Peharec Štefanić P, Koffler T, Adler G, Bar-Zvi D. Chloroplasts of salt-grown Arabidopsis seedlings are impaired in structure, genome copy number and transcript levels. PLoS ONE. 2013;8:e82548.

66. Gao H-J, Yang H-Y, Bai J-P, Liang X-Y, Lou Y, Zhang J-L. Ultrastructural and physiological responses of potato (Solanum tuberosum L.) plantlets to gradient saline stress. Front Plant Sci. 2015;5:787.

67. Oi T, Enomoto S, Nakao T, Arai S, Yamane K, Taniguchi M. Three-dimensional ultrastructural change of chloroplasts in rice mesophyll cells responding to salt stress. Ann Bot. 2020;125:833–40.

68. Fouda H, Sofy M. Effect of biological synthesis of nanoparticles from *Penicillium Chrysogenum* as well as traditional salt and chemical nanoparticles of zinc on canola plant oil productivity and metabolic. Egypt J Chem. 2022;65:507–16.

69. Chuartzman SG, Nevo R, Shimoni E, Charuvi D, Kiss V, Ohad I. Thylakoid membrane remodeling during state transitions in Arabidopsis. Plant Cell. 2008;20:1029–39.

70. Zhao X, Zhang Y, Long T, Wang S, Yang J. Regulation mechanism of plant pigments biosynthesis: anthocyanins, carotenoids, and betalains. Metabolites. 2022;12:871.

71. Manaa A, Goussi R, Derbali W, Cantamessa S, Abdelly C, Barbato R. Salinity tolerance of quinoa (*Chenopodium quinoa* Willd) as assessed by chloroplast ultrastructure and photosynthetic performance. Environ Exp Bot. 2019;162:103–14.

72. Rizwan M, Mostofa MG, Ahmad MZ, Zhou Y, Adeel M, Mehmood S. Hydrogen sulfide enhances rice tolerance to nickel through the prevention of chloroplast damage and the improvement of nitrogen metabolism under excessive nickel. Plant Physiol Biochem. 2019;138:100–11.

73. Chen J, Wu F-H, Shang Y-T, Wang W-H, Hu W-J, Simon M. Hydrogen sulfide improves adaptation of *Zea mays* seedlings to iron deficiency. J Exp Bot. 2015;66:6605–22.

74. Liu F, Fu X, Wu G, Feng Y, Li F, Bi H. Hydrogen peroxide is involved in hydrogen sulfide-induced carbon assimilation and photoprotection in cucumber seedlings. Environ Exp Bot. 2020;175:104052.

75. Parveen M, Asaeda T, Rashid MH. Hydrogen sulfide induced growth, photosynthesis and biochemical responses in three submerged macrophytes. Flora. 2017;230:1–11.

76. Dai H, Xu Y, Zhao L, Shan C. Alleviation of copper toxicity on chloroplast antioxidant capacity and photosystem II photochemistry of wheat by hydrogen sulfide. Brazil J Bot. 2016;39:787–93.

77. Wang C, Deng Y, Liu Z, Liao W. Hydrogen sulfide in plants: crosstalk with other signal molecules in response to abiotic stresses. Int J Mol Sci. 2021;22:12068.

78. Raju AD, Prasad SM. Hydrogen sulfide implications on easing NaCl induced toxicity in eggplant and tomato seedlings. Plant Physiol Biochem. 2021;164:173–84.

79. Salesse-Smith CE, Sharwood RE, Busch FA, Kromdijk J, Bardal V, Stern DB. Overexpression of Rubisco subunits with RAF1 increases Rubisco content in maize. Nat Plants. 2018;4:802–10.

80. Zhang W, Wang L, Zhang L, Kong X, Zhang J, Wang X. H_2S-mediated balance regulation of stomatal and non-stomatal factors responding to drought stress in Chinese cabbage. Hortic Res. 2023;10:uhac284.

81. Shi H, Ye T, Chan Z. Exogenous application of hydrogen sulfide donor sodium hydrosulfide enhanced multiple abiotic stress tolerance in bermudagrass (*Cynodon dactylon* (L). Pers). Plant Physiol Biochem. 2013;71:226–34.

82. Raju AD, Prasad SM. Hydrogen sulfide regulates NaCl tolerance in brinjal and tomato seedlings by Na^+/K^+ homeostasis and nitrogen metabolism. Plant Stress. 2023;7:100129.

83. Liu H, Chong P, Liu Z, Bao X, Tan B. Exogenous hydrogen sulfide improves salt stress tolerance of Reaumuria Soongorica seedlings by regulating active oxygen metabolism. Peer J. 2023;11:e15881.

84. Alamer KH. Exogenous hydrogen sulfide supplementation alleviates the salinity-stress-mediated growth decline in wheat (*Triticum aestivum* L.) by modulating tolerance mechanisms. Plants. 2023;12:3464.

85. Jia W, Wang Y, Zhang S, Zhang J. Salt-stress-induced ABA accumulation is more sensitively triggered in roots than in shoots. J Exp Bot. 2002;53:2201–6.

86. Mäkelä P, Munns R, Colmer TD, Peltonen-Sainio P. Growth of tomato and an ABA-deficient mutant (sitiens) under saline conditions. Physiol Plant. 2003;117:58–63.

87. Hosseinifard M, Stefaniak S, Ghorbani Javid M, Soltani E, Wojtyla Ł, Garnczarska M. Contribution of exogenous proline to abiotic stresses tolerance in plants: a review. Int J Mol Sci. 2022;23:5186.

88. Liu Y-L, Shen Z-J, Simon M, Li H, Ma D-N, Zhu X-Y. Comparative proteomic analysis reveals the regulatory effects of H2S on salt tolerance of mangrove plant *Kandelia Obovata*. Int J Mol Sci. 2019;21:118.

89. Turan M, Ekinci M, Kul R, Boynueyri FG, Yildirim E. Mitigation of salinity stress in cucumber seedlings by exogenous hydrogen sulfide. J Plant Res. 2022;135:517–29.

90. Bennici A, Tani C. Ultrastructural characteristics of callus cells of *Nicotiana tabacum* L. var. BELW3 grown in presence of NaCl. Caryologia. 2012;65:72–81.

91. Kim I, Park S. Ultrastructural characteristics of three chenopod halophytes lacking salt excretion structures. J Plant Biol. 2010;53:314–20.

92. Beri A, Sharma R. Nickel toxicity to photosynthetic attributes in the leaves of lentil (*Lens Culnaris* Medic. Masar). Int J Appl Res. 2016;2:239–42.

93. Rengifo E, Urich R, Herrera A. Water relations and leaf anatomy of the tropical species, *Jatropha Gossypifolia* and *Alternanthera crucis*, grown under an elevated CO_2 concentration. Photosynthetica. 2002;40:397–403.

94. Cao X, Jin X, Zhang X, Li Y, Wang C, Wang X. Morphogenesis of endoplasmic reticulum membrane-invaginated vesicles during beet black scorch virus infection: role of auxiliary replication protein and new implications of three-dimensional architecture. J Virol. 2015;89:6184–95.

95. Spurr AR. A low-viscosity epoxy resin embedding medium for electron microscopy. J Ultrastruct Res. 1969;26:31–43.

96. Metzner H, Rau H, Senger H. Untersuchungen zur synchronisierbarkeit einzelner pigmentmangel-mutanten Von Chlorella. Planta. 1965;65:186–94.

97. Xu Y, Guerra LT, Li Z, Ludwig M, Dismukes GC, Bryant DA. Altered carbohydrate metabolism in glycogen synthase mutants of Synechococcus sp. strain PCC 7002: cell factories for soluble sugars. Metab Eng. 2013;16:56–67.

98. Bradford MM. A rapid and sensitive method for the quantitation of microgram quantities of protein utilizing the principle of protein-dye binding. Anal Biochem. 1976;72:248–54.

99. Muting D, Kaiser E. Quantitative estimation of α-amino N in biological material by the ninhydrin reaction. Hoppe-Seyler's Z fur Physiol Chemie. 1963;332:276–81.

100. Carillo P, Gibbon Y, Protocol. Extraction and determination of proline. Protocols in ecological & environmental plant physiology. 2011. Available online at http://prometheuswiki.publish.csiro.au/tikiindex.php?page=PROTOCOL%3A +Extraction+and+determination+of+proline.

101. Almeida Trapp M, De Souza GD, Rodrigues-Filho E, Boland W, Mithöfer A. Validated method for phytohormone quantification in plants. Front Plant Sci. 2014;5:417.

102. Pan Y, Seymour GB, Lu C, Hu Z, Chen X, Chen G. An ethylene response factor (ERF5) promoting adaptation to drought and salt tolerance in tomato. Plant Cell Rep. 2012;31:349–60.

103. Sairam RK, Rao KV, Srivastava GC. Differential response of wheat genotypes to long term salinity stress in relation to oxidative stress, antioxidant activity and osmolyte concentration. Plant Sci. 2002;163:1037–46.

104. Livak KJ, Schmittgen TD. Analysis of relative gene expression data using real-time quantitative PCR and the 2 – ΔΔCT method. Methods. 2001;25:402–8.

Publisher's Note